

PACS numbers: 42.25.Fx; 42.25.Ja; 78.35+c; 78.67.–n
DOI: 10.1070/QE2014v044n07ABEH015482

Depolarisation of light scattered by disperse systems of low-dimensional potassium polytitanate nanoparticles in the fundamental absorption band

D.A. Zimnyakov, S.A. Yuvchenko, A.B. Pravdin, V.I. Kochubey,
A.V. Gorokhovsky, E.V. Tretyachenko, A.I. Kunitsky

Abstract. **The results of experimental studies of depolarising properties of disperse systems on the basis of potassium polytitanate nanoplatelets and nanoribbons in the visible and near-UV spectral regions are presented. It is shown that in the fundamental absorption band of the nanoparticle material the increase in the depolarisation factor takes place for the radiation scattered perpendicularly to the direction of the probing beam. For nanoribbons a pronounced peak of depolarisation is observed, which is caused by the essential anisotropy of the particles shape and the peculiarities of the behaviour of the material dielectric function. The empirical data are compared with the theoretical results for 'nanodiscs' and 'nanoneedles' with the model dielectric function, corresponding to that obtained from optical constants of the titanium dioxide dielectric function.**

Keywords: *scattering, depolarisation, dielectric function, low-dimensional nanoparticles, potassium polytitanate.*

1. Introduction

One of the fundamental optical properties of disordered disperse nanosystems with small volume fractions of scattering centres is the complete or partial polarisation of initially unpolarised radiation, scattered perpendicularly to the direction of the probing beam propagation. Starting from the seminal papers by Rayleigh, published in 1871 and 1897 in the Philosophical Magazine, the problem of depolarising properties of disordered ensembles of nanoparticles has been repeatedly discussed in numerous papers and monographs (see, e.g., [1–7]). Within the frameworks of the classical concepts of scattering of electromagnetic waves by particles with the dimension smaller than the wavelength, the degree of polarisation of the unpolarised light after its scattering at the right angle by disordered ensemble of similar particles is determined by combinations of the individual particle polarisability tensor components, averaged over all possible orientations of the particle [1–4]. In turn, the polarisability tensor components are determined by the anisotropy of the particle shape and the dielectric constant of its material at the frequency of the probing radiation.

The main results of the classical scattering theory can be summarised as follows. For weakly absorbing particles the minimal value of the depolarisation factor $\Delta_{\min} = I_{\parallel}/I_{\perp}$ for the natural light scattered at the right angle is attained for spherical nanoparticles, the 'nanospheres' ($\Delta = 0$). For quasi-two-dimensional particles ('nanodiscs') the maximal value $\Delta_{\max}$ far from the absorption bands is equal to 2/9, while for quasi-one-dimensional nanoparticles (long nanorods or 'nanoneedles') $\Delta_{\max} = 1/2$. Here $I_{\parallel}$ and $I_{\perp}$ are the components of the scattered light, polarised parallel and perpendicular to the scattering plane, respectively. Below we will use just this notation to determine the experimentally measured and theoretically calculated ratio $I_{\parallel}/I_{\perp}$, although H.C. van de Hulst considered it to be 'somewhat troublesome' ([2], p. 100).

It should be noted that in spite of the abundance of theoretical and experimental studies in the field of optical polarimetry of disperse systems, the influence of the material dielectric function peculiarities in non-spherically shaped nanoparticles on the depolarisation properties of disordered ensembles of such particles is studied insufficiently. Such peculiarities, manifesting themselves in the spectral regions of fundamental absorption of the nanoparticle material in the form of Fröhlich conditions $\varepsilon' + K\varepsilon_m = 0$ [3] or spectral intervals where $\varepsilon' < 0$, can essentially affect the depolarisation factor, increasing it up to the limit value [3] $\Delta = 3/4$ (for polarised probing light) and $\Delta = 6/7$ (for natural probing light). Here ε' is the real part of the particle material permittivity, ε_m is the real value of the permittivity of non-absorbing host medium; K is the coefficient determined by the shape of the particles (e.g., for 'nanodiscs' $K = 0$ and for 'nanoneedles' $K = 1$). In particular, the studies on depolarising properties of noble metal nanorods [8–14] have shown that for the spectral regions of plasmon resonance manifestation and for linearly polarised probing radiation $\Delta \gg 1/3$, the latter value being characteristic for quasi-one-dimensional nanoparticles with large positive values of ε' and zero imaginary part of the permittivity ($\varepsilon'' = 0$).

Such peculiarities of the dielectric function can manifest themselves in the short-wave part of the visible region and in the near UV spectral region, as well as in the case of particles based on high energy-gap semiconductors (e.g., various derivatives of titanium dioxide with the band gap 2.5–3.5 eV). The interest to the investigation of optical properties of such objects is caused, in particular, by the possibility of using them to create novel promising materials for applications in photochemistry [15], solar energetics [16], photobiology and medicine [17], and other fields. Earlier [18, 19] it was found

D.A. Zimnyakov, S.A. Yuvchenko, A.V. Gorokhovsky, E.V. Tretyachenko, A.I. Kunitsky Saratov State Technical University, ul. Politekhnicheskaya 77, 410054 Saratov, Russia; e-mail: zimnykov@mail.ru, yuv-sergej@yandex.ru;
A.B.Pravdin, V.I.Kochubey N.G. Chernyshevsky Saratov State University, ul. Astrakhanskaya 83, 410012 Saratov, Russia; e-mail: pravdinab@mail.ru, Saratov_gu@mail.ru.

Received 2 Ferbruary 2014; revision received 27 March 2014
Kvantovaya Elektronika **44** (7) 670–674 (2014)
Translated by V.L. Derbov

that in the extinction spectra of potassium polytitanate (PPT) nanoplatelets the characteristic peaks arise in the near UV region, caused by the manifestation of Fröhlich resonances at $K \approx 0$. The analysis of the expected behaviour of the PPT dielectric function in the interval of probing radiation wavelengths 200–350 nm basing on the known data on the optical constants of the initial material for the PPT synthesis (titanium dioxide, [20]), and the interpretation of the extinction spectra of the synthesised disperse nanosystems result in a conclusion that in the considered spectral interval ε' possesses essentially negative values.

In the present paper we report the results of the study of depolarising properties of disperse systems based on PPT nanoparticles with lowered dimensionality (nanoplatelets and nanoribbons) in the spectral regions where the abovementioned peculiarities of the particle material dielectric function manifest themselves.

2. Experimental technique and results

Polarisation-dependent spectra of radiation, scattered at the right angle with respect to the direction of probing light propagation by disperse systems of PPT nanoparticles in distilled water with addition of surface-active substances were recorded in the spectral interval 300–600 nm using the LS55 spectrofluorimeter (PerkinElmer). The used samples of nanomaterials were synthesised following the protocol [21] in the melt of salts, processing the titanium oxide powder (atanase 99%, Aldrich, mean particle size 7 μm) in salt melt. The reaction mixture, containing TiO_2 (mass fraction 10%) and the melt, consisting of KOH agreeable to the All-Russian State Standard 24363-80 and KNO_3 agreeable to the All-Russian State Standard 4217-77 (mass fraction 80%), was kept in the alundum crucible in a muffle furnace at the temperature 500 °C during 2 hours. The product was then washed from water-soluble compositions in distilled water taken in the proportion of 40 : 1 to the content of the crucible, filtered using the paper filter Whathman No. 40, centrifuged and dried at 40 °C.

A part of the produced PPT samples were subjected to the additional thermal procession in the alundum crucible in the muffle furnace during 1 hour at the temperature 600 °C, which was lower than the temperature of the PPT crystallisation that varies from 700 to 780 °C depending on the content of TiO_2 and K_2O.

To provide exfoliation and deagglomeration of nanoparticles, the powders of the initial and thermally modified PPT were processed in the aqueous solutions of surface-active substance (SAS) (non-ionogenic SAS OP-10, the polyethylene glycol-monoalkyl phenyl ether). The procession was lasted two days and was implemented at room temperature using the aqueous solution of SAS (H_2O : PPT : SAS = 2000 : 100 : 1) with stirring. Then the solid sediment was separated using a centrifuge, washed with distilled water and used to prepare the disperse systems of nanoparticles aimed at subsequent spectral and polarisation measurements. In accordance with the results of the energy dispersion analysis, the chemical composition of the synthesised PPT nanoparticles corresponded to the mole ratio $[TiO_2]/[K_2O] = 4.2$. The diffractometer analysis has shown that the synthesised PPT without thermal procession is a quasi-amorphous substance with weakly ordered structure; in the obtained diffraction patterns only the reflection typical for layered structures could be seen [22]. After the thermal processing the ordering degree of the PPT structure slightly increases, but no essential changes in the character of the diffraction patterns occur.

The analysis of the produced PPT nanoparticles shape using the transmission electron microscope iCE-3500 has shown that non-modified PPT nanoparticles have lamellar structure (Fig. 1a) and the mean lateral size ~0.34 μm with the thickness 10–30 nm. Thermally modified PPT particles have ribbon-like shape (Fig. 1,b), with the length and the width of the synthesised ribbons equal to ~1.3 μm and ~0.2 μm, respectively, and the thickness varying from 10 to 20 nm. Therefore, the form-factor (the ratio of length to width) for the synthesised nanoribbons is ~6.5.

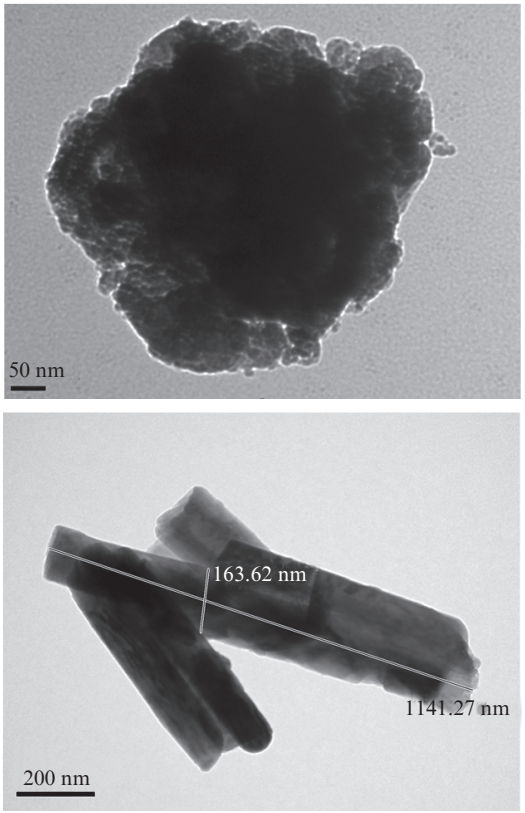

Figure 1. Images of PPT nanoplatelets (a) and a group of nanoribbons (b) obtained using the transmission electron microscopy.

For spectral-polarisation measurements during the scattering at right angles, we prepared aqueous dispersions of PPT nanoplatelets and nanoribbons with the volume fraction of particles corresponding to the regime of single scattering of probe radiation. To this end, the volume fraction of particles in the samples under study was decreased by dilution with distilled water to achieve an optical density of 0.01–0.02 at a wavelength of 532 nm (cuvette thickness of 10 mm). The spectra of the radiation scattered at right angles were recorded at different orientations of the polariser and analyser axes with respect to the scattering plane: $I_{\perp,\perp}(\lambda)$, $I_{\perp,\parallel}(\lambda)$, $I_{\parallel,\perp}(\lambda)$, $I_{\parallel,\parallel}(\lambda)$ (the subscript $\parallel$ corresponds to the axis parallel to the scattering plane, and $\perp$ – to the axis perpendicular to the scattering plane; the first subscript corresponds to the polariser, the second – to the analyser). Spectra $I_{\parallel,\perp}(\lambda)$, $I_{\parallel,\parallel}(\lambda)$ played a supporting role and were used to calculate the wavelength-dependent normalisation factor $K(\lambda) = I_{\parallel,\perp}(\lambda)/I_{\parallel,\parallel}(\lambda)$, taking into account the different sensitivity of the spectrofluorimeter dur-

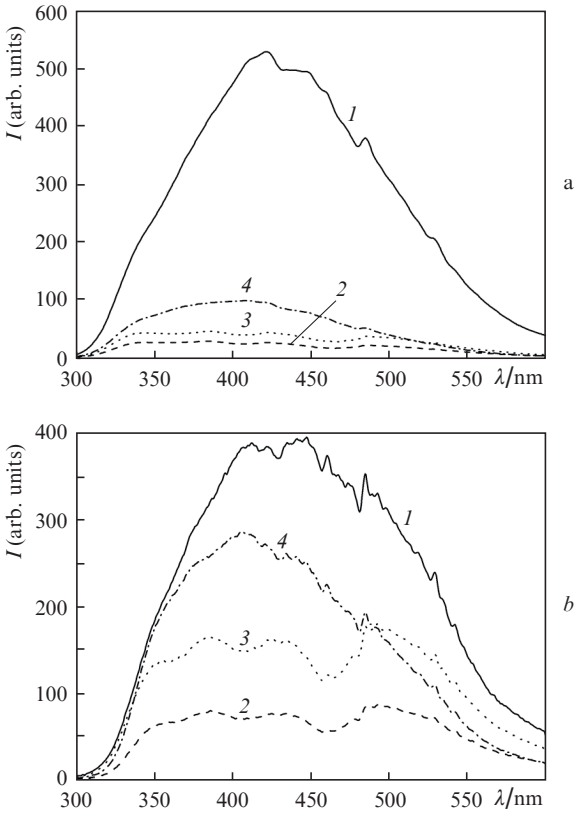

Figure 2. Scattering spectra of aqueous suspensions of nanoplatelets (a) and nanoribbons (b), obtained in the experiment: (*1*) $I_{\perp,\perp}(\lambda)$; (*2*) $I_{\perp,\parallel}(\lambda)$; (*3*) $I_{\parallel,\parallel}(\lambda)$; (*4*) $I_{\parallel,\perp}(\lambda)$.

ing the registration of vertically and horizontally polarised components of scattered light. Figure 2 shows the experimentally obtained dependences of $I_{\perp,\perp}(\lambda)$, $I_{\perp,\parallel}(\lambda)$, $I_{\parallel,\perp}(\lambda)$, and $I_{\parallel,\parallel}(\lambda)$ for PPT nanoplatelets and nanoribbons.

The analysis of scattering matrices for disordered ensembles of nonspherical particles [2] shows that when probe radiation, initially polarised in the scattering plane, is scattered at the right angle, the intensities of the scattered components with parallel and perpendicular polarisations are equal, and the difference in the recorded values of $I_{\parallel,\perp}(\lambda)$ and $I_{\parallel,\parallel}(\lambda)$ is caused only by the instrumental error, introduced by the spectrofluorimeter optical scheme. Using the obtained dependence of $K(\lambda)$, the correction of spectra was performed, $\tilde{I}_{\perp,\perp}(\lambda)$, $\tilde{I}_{\perp,\parallel}(\lambda) \leftarrow I_{\perp,\perp}(\lambda)/K(\lambda)$, $I_{\perp,\parallel}(\lambda)$, after which based on the obtained data the dependences $\Delta(\lambda) = \tilde{I}_{\perp,\parallel}(\lambda)/\tilde{I}_{\perp,\perp}(\lambda)$ have been restored. Figure 3 presents the spectral dependences of the depolarisation factor, calculated using the data of Fig. 2.

3. Discussion of experimental results

It is interesting to compare the obtained experimental data on the depolarising properties of suspensions of PPT nanoplatelets and nanoribbons with the theoretical values of the depolarisation factor for disordered ensembles of quasi-two-dimensional and quasi-one-dimensional nanoparticles ('nanodiscs' and 'nanoneedles', respectively, that can be considered as extremely oblate or extremely prolate ellipsoids of rotation) with the model dielectric function, the frequency dependence of which is qualitatively resembling the frequency dependence of dielectric functions of the synthesised nanomaterials. The light polarisation state after single scattering by a

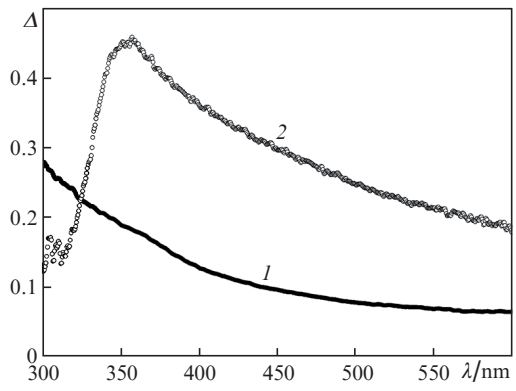

Figure 3. Spectral dependences of the depolarisation factor $\Delta(\lambda)$ for PPT nanoplatelets (*1*) and nanoribbons (*2*), obtained from the experimental data of Fig. 2.

disordered ensemble of ellipsoidal particles, small compared to the wavelength, is determined by the ratio $M = K_1/K_2$ of the following combinations of ensemble-averaged principal values of the polarisability tensor of the particles [2–4]

$$K_1 = \mathrm{Re}\{\alpha_1^*\alpha_2 + \alpha_1^*\alpha_3 + \alpha_2^*\alpha_3\},$$
$$K_2 = |\alpha_1|^2 + |\alpha_2|^2 + |\alpha_3|^2 \quad (1)$$

For further analysis let us introduce the complex parameter $\gamma = \varepsilon_m/(\varepsilon - \varepsilon_m)$, where ε is the complex value of the particle material permittivity (the particle material is assumed to be homogeneous and isotropic). This allows the presentation of the polarisability tensor principal components α_j in the following way:

$$\alpha_j = \frac{4}{3}\pi abc\frac{1}{\gamma + L_j}, \quad (2)$$

where L_j is the so-called geometric factor [2, 3]; and a, b, and c are the lengths of the ellipsoid axes.

This form of the polarisability tensor principal values, after substituting them into Eqm (1) and some transformations, allows expressing the parameter M in the form of a ratio of two polynomials of the 4th order with respect to $\mathrm{Re}\gamma$ and $\mathrm{Im}\gamma$ with the coefficients depending on L_1, L_2, and L_3. For strongly oblate and strongly prolate particles that allow representation with oblate and prolate ellipsoids of rotation, $L_1 \approx L_2 = L$, $L_3 \approx 1 - 2L$. When probing a disperse system with natural (unpolarised) light, the depolarisation factor for the light scattered at the right angle is expressed as [2, 3]

$$\Delta = \frac{2 - 2M}{4 + M}, \quad (3)$$

and for linearly polarised probing light with the electric field vector, oriented perpendicularly to the scattering plane (this case corresponds to the conditions of our experiment)

$$\Delta = \frac{1 - M}{3 + 2M}. \quad (4)$$

Expressions (1)–(4) allow a quantitative analysis of the spectral dependence of the depolarisation degree of light scat-

tered at the angle 90° by small particles of various shape with the known spectral dependences $\mathrm{Re}\gamma(\lambda)$ and $\mathrm{Im}\gamma(\lambda)$. For 'nanodiscs' ($L_1 = L_2 = 0$, $L_3 = 1$))

$$M = \frac{3\,\mathrm{Re}^4\gamma + 4\,\mathrm{Re}^3\gamma + \mathrm{Re}^2\gamma + 3\,\mathrm{Im}^4\gamma}{3\,\mathrm{Re}^4\gamma + 4\,\mathrm{Re}^3\gamma + 2\,\mathrm{Re}^2\gamma + 3\,\mathrm{Im}^4\gamma} \rightarrow$$
$$\rightarrow \frac{+\,\mathrm{Im}^2\gamma + 6\,\mathrm{Re}^2\gamma\,\mathrm{Im}^2\gamma + 4\,\mathrm{Re}\gamma\,\mathrm{Im}^2\gamma}{+\,2\,\mathrm{Im}^2\gamma + 6\,\mathrm{Re}^2\gamma\,\mathrm{Im}^2\gamma + 4\,\mathrm{Re}\gamma\,\mathrm{Im}^2\gamma}, \quad (5)$$

and for 'nanoneedles' ($L_1 = L_2 = 0.5$, $L_3 = 0$)

$$M = \frac{3\,\mathrm{Re}^4\gamma + 4\,\mathrm{Re}^3\gamma + (7/4)\,\mathrm{Re}^2\gamma + (1/4)\,\mathrm{Re}\gamma + 3\,\mathrm{Im}^4\gamma}{3\,\mathrm{Re}^4\gamma + 4\,\mathrm{Re}^3\gamma + 2\,\mathrm{Re}^2\gamma + (1/2)\,\mathrm{Re}\gamma + 3\,\mathrm{Im}^4\gamma} \rightarrow$$
$$\rightarrow \frac{+\,(3/4)\,\mathrm{Im}^2\gamma + 6\,\mathrm{Re}^2\gamma\,\mathrm{Im}^2\gamma + 4\,\mathrm{Re}\gamma\,\mathrm{Im}^2\gamma}{+\,\mathrm{Im}^2\gamma + 6\,\mathrm{Re}^2\gamma\,\mathrm{Im}^2\gamma + 4\,\mathrm{Re}\gamma\,\mathrm{Im}^2\gamma + (1/16)}. \quad (6)$$

For nonspherical nonabsorbing particles with $\varepsilon' \gg \varepsilon_\mathrm{m}$ the values of γ satisfy the conditions $\mathrm{Im}\gamma = 0$, $\mathrm{Re}\gamma \ll 1$ and, therefore, $M = 0.5$ for 'nanodiscs' and $M = 0$ for 'nanoneedles'. In the fundamental absorption band of the nanoparticle material, where significant variations of $\mathrm{Re}\gamma$ and $\mathrm{Im}\gamma$ occur under the variation of the probing radiation wavelength and, in particular, $\mathrm{Re}\gamma$ can take negative values, the value of M for nonspherical quasi-two-dimensional and quasi-one-dimensional particles will essentially differ from the values presented above. In the case $\mathrm{Re}\gamma < 0$ an essential influence of the variations of M with varying λ will be exerted by the terms, linear and cubic in $\mathrm{Re}\gamma$.

As a model dielectric function for 'nanodiscs' and 'nanoneedles' we took the function $\varepsilon(\lambda)$, corresponding to the spectral dependence of the optical constants n and k, presented in Ref. [20] for the bulk titanium dioxide (the source material used in the synthesis of PPT nanoplatelets and nanoribbons). A similar approach has been used earlier in the analysis of the extinction spectra of PPT nanoplatelets in the near UV region [18, 19]. It was found that the frequencies, corresponding to the experimentally observed extinction peaks that are expected to satisfy the Fröhlich conditions for nanodiscs ($\varepsilon' \approx 0$) [3] demonstrate satisfactory agreement with the frequency values, for which the real part of the dielectric function of the bulk titanium dioxide is close to zero. In further analysis the model values of $\mathrm{Re}\gamma$ and $\mathrm{Im}\gamma$ for the initial bulk material were calculated in correspondence with the following expressions

$$\mathrm{Re}\gamma(\lambda) = \frac{n_\mathrm{m}^2(\lambda)[n^2(\lambda) - k^2(\lambda) - n_\mathrm{m}^2(\lambda)]}{[n^2(\lambda) - k^2(\lambda) - n_\mathrm{m}^2(\lambda)]^2 + 4n^2(\lambda)k^2(\lambda)},$$
$$\mathrm{Im}\gamma(\lambda) = \frac{2n_\mathrm{m}(\lambda)n(\lambda)k(\lambda)}{[n^2(\lambda) - k^2(\lambda) - n_\mathrm{m}^2(\lambda)]^2 + 4n^2(\lambda)k^2(\lambda)}, \quad (7)$$

where $n_\mathrm{m}(\lambda)$ is the refractive index of the nonabsorbing host medium (distilled water), containing the particles. Figure 4b presents the obtained model dependences $\mathrm{Re}\gamma(\lambda)$ and $\mathrm{Im}\gamma(\lambda)$, and Fig. 4a shows the corresponding model dependences $M(\lambda)$ for 'nanodiscs' and 'nanoneedles'. Note that for 'nanoneedles' with the model dielectric function in the vicinity of $\lambda \approx 265$ nm a negative value of M is attained, close to the limit one ($M = -0.5$ [3]).

Figure 5 presents the spectral dependences $\Delta(\lambda)$, calculated using the data of Fig. 4 for probing disperse systems

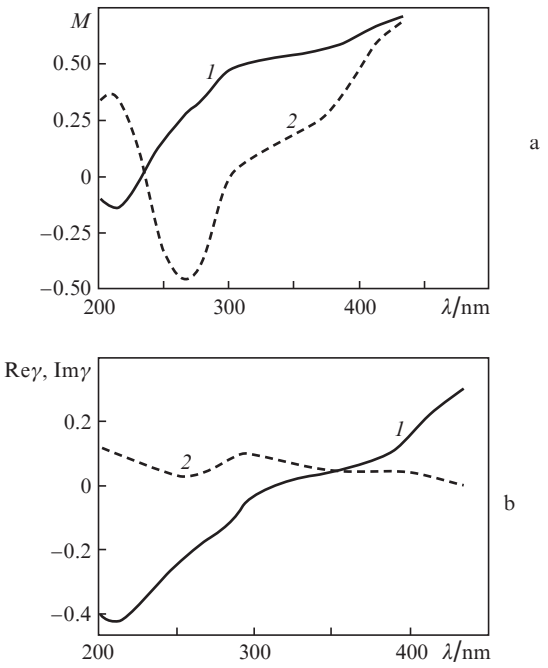

Figure 4. Model spectral dependences of the parameter M for 'nanodiscs' (*1*) and 'nanoneedles' (*2*) (a) and model spectral dependences of $\mathrm{Re}\gamma$ (*1*) and $\mathrm{Im}\gamma$ (*2*) for the material with the dielectric function, adopted from Ref. [16] (b).

with linearly polarised light [Eqn (4)]. Note that there are general tendencies in the behaviour of the empirical dependences $\Delta(\lambda)$ for PPT nanoplatelets and nanoribbons (see Fig. 3), on the one hand, and the derived model dependences, on the other hand. They consist in the presence of pronounced peaks of the depolarisation factor in the case of 'nanoneedles' and PPT nanoribbons, and the monotonic growth of Δ for 'nanodiscs' (Fig. 5) and PPT nanoplatelets (Fig. 3) with decreasing wavelength within the limits of the analysed spectral intervals. At the same time, the model and empirical dependences are characterised by essential quantitative differences that manifest themselves, first of all, in a systematic shift of the model values $\Delta(\lambda)$ towards the short-wavelength region with respect to the experimentally obtained values of the depolarisation factor, and also in essentially smaller peak values of Δ for nanoribbons in comparison with the model values for 'nanoneedles'.

The shift of the model values of the depolarisation factor towards the short-wave region with respect to the empirical

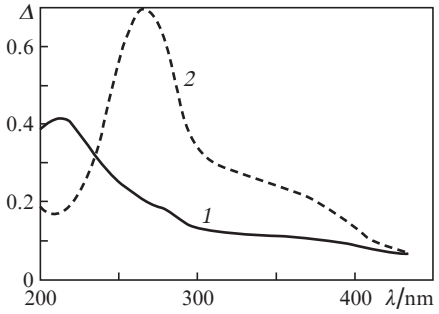

Figure 5. Model spectral dependences of the depolarisation factor for 'nanodiscs' (*1*) and 'nanoneedles' (*2*).

data can be interpreted as a consequence of the difference in electron structure and, therefore, in the spectra of dielectric functions for the synthesised PPT nanoplatelets and nanoribbons and the source material, caused by the difference in their chemical composition. Moreover, the high density of structure defects in the synthesised low-dimensional nanomaterials should lead to the appearance of pronounced Urbach 'tails' and essentially affect the effective values of the band gap width for them. The observed shift of the model values towards higher frequencies with respect to the empirical data seems somewhat unexpected, keeping in mind the abovementioned data of Refs [18, 19] on the localisation of the extinction peaks of the PPT nanoplatelets at the wavelengths, approximately corresponding to the Fröhlich condition $\varepsilon' \approx 0$. However, in contrast to the scattering and absorption cross section, averaged over all possible orientations of the particles, the Fröhlich resonances do not manifest themselves in such an obvious way in the spectral dependences of the depolarisation factor. It should be also noted that small deviations of the effective values of ε' and ε'' for the synthesised nanoparticles from the analogous values for the source material may essentially affect $\mathrm{Re}\gamma(\lambda)$ and $\mathrm{Im}\gamma(\lambda)$ without any significant change in the characteristic wavelength at which $\varepsilon' \approx 0$.

The essentially smaller peak values of Δ for PPT nanoribbons in comparison with the model values for long nanorods, or 'nanoneedles', can be interpreted as a consequence of the finite form-factor values of the nanoribbons that do not exceed 6–8 for the samples studied. It is also worth noting that the peak model value of Δ for 'nanoneedles' is attained at $\lambda \approx 265$ nm, which approximately corresponds to the region of the lowest negative values of the used model dielectric function, where $\varepsilon'/\varepsilon_m \approx -4 \div -5$. Note, that for long nanorods the resonance excitation of the Fröhlich mode in the direction of the rod axis is attained at $\varepsilon' \to -\infty$, while the resonance excitation of the mode in the direction, orthogonal to the axis of the rod, occurs at $\varepsilon' \to -\varepsilon_m$ [3]. One can suppose that the growth of the depolarisation factor is to some extent determined by the increase in the efficiency of the longitudinal Fröhlich mode excitation in the region of essentially negative values of ε'.

4. Conclusions

Thus, for the studied disperse systems of low-dimensional particles on the basis of high energy-gap semiconductor materials a typical feature is the essential growth of the depolarisation factor in the spectral region, corresponding to fundamental absorption of the nanoparticle material. For particles with essential shape anisotropy, manifesting itself in significantly greater value of one characteristic dimension in comparison with other two dimensions, a pronounced peak of the depolarisation factor is observed. The comparison of the experimental data for potassium polytitanate nanoribbons with the results of modelling for titanium dioxide nanoneedles allows a hypothesis that the height of this peak is somewhat indicating 'one-dimensionality' of nanoparticles, attaining the maximum in the limit cases $L_1 \to 0.5$, $L_2 \to 0.5$, $L_3 \to 0$, other conditions being equal. The obtained results can be used to develop a spectral polarisation method for the analysis of morphology features in disperse nanosystems.

Acknowledgements. The work was supported by the Russian Foundation for Basic Research (Grant No. 13-02-90468).

References

1. Kerker M. *The Scattering of Light and Other Electromagnetic Radiation* (New York: Acad. Press, 1969).
2. Van de Hulst H.C. *Light Scattering by Small Particles* (New York: John Wiley & Sons, 1957; Moscow: IL, 1961).
3. Bohren C.F., Huffman D.R. *Absorption and scattering of light by small particles* (New York: John Wiley & Sons, 1983; Moscow: Mir, 1986).
4. Landau L.D., Lifshits E.M. *Electrodynamics of Continuous Media* (Oxford: Pergamon Press, 1984; Moscow: Nauka, 1982).
5. Heller W., Nakagaki M. *J. Chem. Phys*., **61**, 3619 (1974).
6. Mehta R.V., Shah H.S., Desai J.N. *J. Colloid Interface Sci*., **36**, 80 (1971).
7. Ravey J.-C. *J. Colloid Interface Sci*., **56**, 540 (1976).
8. Khlebtsov N.G., Melnikov A.G., Bogatyrev V.A., Dykman L.A., Alekseeva A.V., Trachuk L.A., Khlebtsov B.N. *J. Phys. Chem. B*, **109**, 13578 (2005).
9. Gryczynski Z., Lukomska J., Lakowicz J.R., Matveeva E.G., Gryczynski I. *Chem Phys Lett*., **421**, 189 (2006).
10. Calander N., Gryczynski I., Gryczynski Z. *Chem. Phys. Lett*., **434**, 326 (2007).
11. Khlebtsov B.N., Khanadeev V.A., Khlebtsov N.G. *J. Phys. Chem. C*, **112**, 12760 (2008).
12. Khlebtsov N.G. *J. Nanophoton*., **4**, 041587 (2010).
13. Khlebtsov B., Khanadeev V., Khlebtsov N. *Phys. Chem. Chem. Phys*., **12**, 3210 (2010).
14. Khlebtsov B.N., Khanadeev V.A., Khlebtsov N.G. *Phys. Chem. Chem. Phys*., **16**, doi 10.1039/C3CP55414G (2014).
15. Peilin Z., Xiangwen L., Shu Y., Tsugio S. *Appl. Catalysis B: Environmental*, **93**, 299 (2010).
16. Colodrero S., Calvo M.E., Mîguez H., in: *Solar Energy* (Ed. by R.D.Rugescu) (Croatia: INTECH, 2010, p. 413).
17. Popov A.P., Priezzhev A.V., Lademann J., Myllylä R. *J. Phys. D: Appl. Phys*., **38**, 2564 (2005).
18. Zimnyakov D.A., Ushakova O.V., Gorokhovsky A.V., Tretyachenko E.V., Isaeva E.A., Isaeva A.A., Pravdin A.B. *Appl. Opt*., **51**, 3675 (2012).
19. Zimnyakov D.A., Gorokhovsky A.V., Tretyachenko E.V., Ushakova O.V., Isaeva E.A., Isaeva A.A. *Opt. Mater*., **34**, 1865 (2012).
20. http://www.ioffe.ru/SVA/NSM/nk/Oxides/Gif/tio2.gif.
21. Sanchez-Monjaras T., Gorokhovsky A.V., Escalante-Garcia J.I. *J. Am. Ceram. Soc*., **91**, 3058 (2008).
22. Kim T.W., Ha H.-W., Paek M.-J., Hyun S.-H., Baek I.-H., Choy J.-H., Hwang S.-J. *J. Phys. Chem. C*, **112**, 14853 (2008).